Organic vapor adsorption on in situ grown carbon nanotube films

Bosnick, Ken; Ban, Shuai; Hiebert, Wayne; Shi, Zheng; Huang, Cheng; Lister, Ryan; Mleczko, Michal

Publisher's version / Version de l'éditeur:
https://doi.org/10.1016/j.carbon.2011.04.067
Carbon, 49, 11, pp. 3639-3644, 2011-05-05

CARBON 49 (2011) 3639–3644

available at www.sciencedirect.com

ScienceDirect

journal homepage: www.elsevier.com/locate/carbon

Organic vapor adsorption on in situ grown carbon nanotube films

Ken Bosnick [a,*], *Shuai Ban* [b], *Wayne Hiebert* [a], *Zheng Shi* [b], *Cheng Huang* [b], *Ryan Lister* [a], *Michal Mleczko* [a]

[a] *National Institute for Nanotechnology, National Research Council Canada, 11421 Saskatchewan Drive, Edmonton, Alberta, Canada T6G 2M9*

[b] *Institute for Fuel Cell Innovation, National Research Council Canada, 4250 Wesbrook Mall, Vancouver, British Columbia, Canada V6T 1W5*

ARTICLE INFO

Article history:
Received 17 March 2011
Accepted 29 April 2011
Available online 5 May 2011

ABSTRACT

Organic vapor adsorption isotherms are measured on in situ grown carbon nanotube (CNT) films using piezoelectric $GaPO_4$ crystal microbalances as mass sensing substrates. The isotherms are Type IV and show adsorption/desorption hysteresis, consistent with a porous material. The measured porosity is 2%, a value surprisingly low given an over 90% void volume in the film estimated from density considerations. At low pressures ($p/p_0 < 0.25$) the isotherm is well fit by the Freundlich model and at intermediate pressures ($p/p_0 = 0.1–0.4$) by the Brunauer, Emmett, Teller (BET) model. Monte Carlo simulations show three consecutive adsorption processes: filling of the intratube micropores at low pressures, monolayer coverage of the CNT external surface at intermediate pressures, and capillary condensation in the intertube mesopores at high pressures. The simulation results validate the use of the BET model for surface area analysis in the experimental system. The average total accessible surface area is found to be 180 ± 100 mm^2 and the specific surface area is estimated to be 45 ± 25 m^2/g. Further engineering of the CNT film microstructure should lead to much higher surface areas.

1. Introduction

Vertically aligned carbon nanotube (VACNT) films are among the morphologies of carbon nanotubes (CNT) with the most potential for technological exploitation [1]. These films can be grown on various substrates with a high level of control over the film dimensions (e.g. length, CNT diameter, film density, etc.) [2,3]. The films appear highly porous with a large surface area suggesting they may be useful for such applications as supports for catalyst particles, separation media, electrochemical electrodes, and sensors. However, accurate measurements of the porosity of the film are needed before these applications can be realized. In general, porosity is measured by following the change in some property of the porous material as the pores are filled with an adsorbate under equilibrium conditions. Measurement of porosity for bulk materials is a mature science [4]. However, bulk techniques are generally not sensitive enough to measure the porosity of a thin film on a support material.

A number of techniques have been demonstrated for measuring the porosity of thin films, with ellipsometric porosimetry (EP) emerging as dominant [5,6]. With EP, the refractive index of the material is measured by ellipsometry as the pores are filled with the adsorbate to produce the isotherm. Ellipsometry is, however, restricted in its suitability to transparent films. VACNT films hold the record as the darkest (most light absorbing) material ever made, and hence EP will not work [7]. Other "beam" techniques for thin film

* *Corresponding author:*
E-mail address: ken.bosnick@nrc.ca (K. Bosnick).
0008-6223/$ - see front matter
doi:10.1016/j.carbon.2011.04.067

porosimetry have also been demonstrated (e.g. X-ray reflectance porosimetry, small angle neutron scattering porosimetry, etc.) [6,8]. While these techniques may be compatible with VACNT films, they are not commonly available.

Thin film "gravimetric" techniques involve depositing the porous thin film directly on a piezoelectric quartz crystal and measuring the mass of the film as the pores are filled via the resonant frequency of the crystal [6,9]. Piezoelectric quartz crystals are, however, damaged due to "twinning" at high temperatures and hence are restricted to temperatures below about 300 °C [10]. While some plasma enhanced chemical vapor deposition (CVD) processes operate at these temperatures, more common thermal CVD processes generally work at much higher temperatures, including the growth of VACNT films by thermal CVD (650 °C).

There are alternative mass sensing substrates that are compatible with high temperature processing, including piezoelectric $GaPO_4$ crystals [11] and silicon MEMS resonators. To our knowledge, neither of these have previously been used for thin film porosimetry measurements. Piezoelectric $GaPO_4$ crystals were developed specifically as high-temperature alternatives to piezoelectric quartz crystals for quartz crystal microbalances and have the advantage that they work well at ambient pressures. Silicon MEMS resonators are routinely fabricated and we have shown that VACNT films can be deposited directly on them. MEMS resonators do, however, suffer from decreased performance at ambient pressures, which adds additional challenges to their use for porosimetry. In this paper we report on the in situ growth of VACNT films on piezoelectric $GaPO_4$ crystals and the use of these hybrid devices to measure organic vapor adsorption on the VACNT film. Monte Carlo simulations are performed to understand the mechanistic details of the resulting isotherms.

2. Experiment and simulation details

Piezoelectric $GaPO_4$ crystals are purchased from Tangidyne Corp (R-30 crystal, Pt/Ti electrodes, ~0.3 ng/Hz). Catalyst is evaporated as a 7 mm diameter patch on one side of the crystal (200 nm SiO_2, 3 nm Cr, 1 nm Ni, 1 nm Fe). VACNT films are grown in situ on the crystals as reported previously [2], with a 90 min reduction cycle and a 20 min growth cycle at 650 °C. The hybrid device is mounted in a flow cell, equipped with pure and saturated argon input lines and an exhaust. The saturated stream is produced by bubbling argon through an adsorbate column. The flow rates are controlled by mass flow controllers. The sorbent partial pressure is controlled by varying the pure and saturated stream flow rates, while keeping a constant total flow of about 150 sccm (with a flow cell volume of about 150 cm^3).

Adsorbate materials [12] are purchased from Sigma–Aldrich and are HPLC grade. The frequency of the crystal is measured using a Sycon Instruments STM-2 thin film thickness monitor; the frequency resolution of the $GaPO_4$ crystals, based on oscillator noise, is 0.06 Hz giving a mass resolution of about 20 pg. The entire porosimetry experiment is automated using a LabView program. Frequency measurements are taken at 30 s intervals and the system is assumed to have reached equilibrium when 240 consecutive measurements show a standard deviation of less than 3 Hz. The experiments are performed at ambient temperature.

The VACNT film thickness is measured using a KLA-Tencor P-10 profilometer. The scanning electron micrograph of the device cross section was obtained on a Hitachi S4800 field emission scanning electron microscope by cleaving a VACNT film device. The mass of the VACNT is estimated from the frequency shift caused by film growth. A reproducible correction of 1.1 μg is used to account for the frequency shift caused by thermal cycling of the crystal in the deposition process.

Simulated adsorption isotherms are calculated using a configurational-bias Monte Carlo simulation in the grand-canonical ensemble [13]. Lennard–Jones interactions are used to describe interactions between the toluene molecules and the carbon nanotube. Toluene is described by an uncharged united atom model with $\sigma_{CH-CH} = 3.88$ Å, $\varepsilon_{CH-CH} = 21$ K, $\sigma_{CH3-CH3} = 3.75$ Å, and $\varepsilon_{CH3-CH3} = 98$ K. The guest–host interactions are $\sigma_{C-CH} = 3.64$ Å, $\varepsilon_{C-CH} = 24.252$ K, $\sigma_{C-CH3} = 3.575$ Å, and $\varepsilon_{C-CH3} = 52.39$ K. All the intermolecular interactions are truncated and shifted at 15 Å. A (10, 10) single-wall CNT (diameter 13.6 Å) is placed in the centre of a 40 Å simulation box. Both the toluene and the CNT are treated as rigid molecules and periodic boundary conditions are applied. A typical simulation consists of at least 4×10^6 cycles. In each cycle, trial moves are attempted to translate, rotate, (partially) regrow a molecule, or exchange a molecule with the reservoir. The number of trial moves per cycle is equal to the number of molecules with a minimum of 20.

3. Results and discussion

A scanning electron micrograph of the cross section of a typical $GaPO_4$ device is shown in Fig. 1. The CNT film clearly grew on the device substrate; however, the substrate may have influenced the morphology of the film compared to that

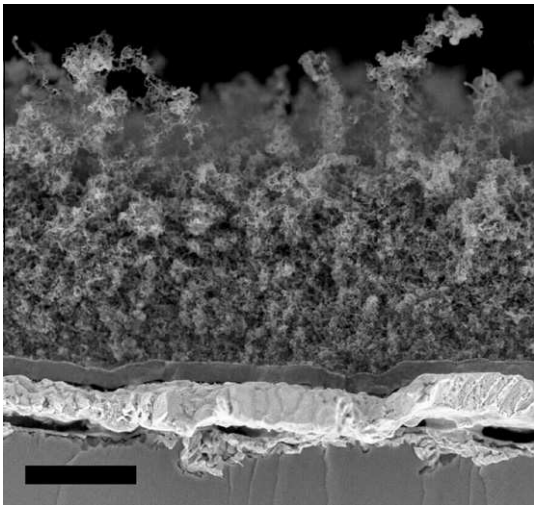

Fig. 1 – FESEM micrograph of the cross section of a VACNT film/$GaPO_4$ device obtained by cleaving the device. The dominant layers in the image are VACNT film, SiO_2, Pt/Ti electrode, and $GaPO_4$ crystal (from the top). The scale bar is 1 μm.

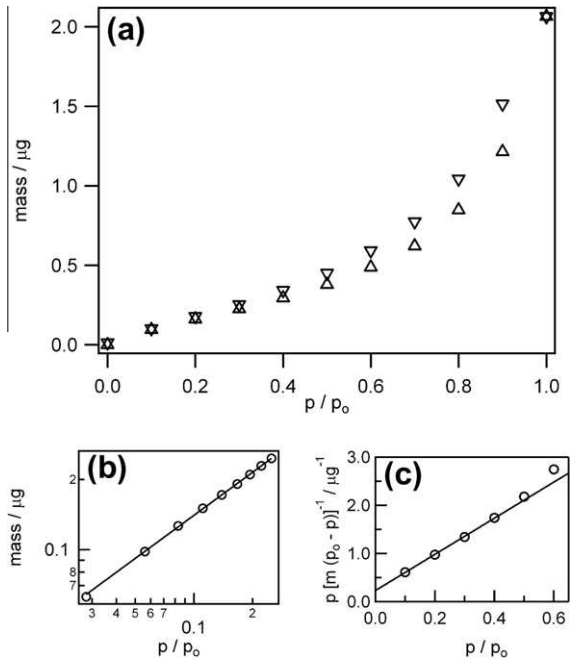

Fig. 2 – (a) Toluene adsorption (Δ) and desorption (▽) isotherms measured on a VACNT film/$GaPO_4$ device. (b) Freundlich plot of the toluene adsorption isotherm. A good fit to the Freundlich model is obtained for $p/p_0 < 0.25$. (c) BET plot of the toluene adsorption isotherm. A good fit to the BET model is obtained for $p/p_0 = 0.1–0.4$.

which is obtained on thermally oxidized silicon wafers with the same catalyst and growth conditions [2]. The SiO_2 layer, the electrode, and the $GaPO_4$ crystal are visible below the VACNT film. The apparent gaps between the layers are a result of the cleaving process. A typical toluene isotherm, measured on a VACNT film/$GaPO_4$ device, is shown in Fig. 2a for both adsorption and desorption directions. The isotherm shows an initial fast rise in mass uptake at low values of p/p_0 (where p is the vapor pressure of the adsorbate and p_0 is the saturation vapor pressure). The mass uptake rate then slows and increases again with increasing p/p_0. This sigmoidal shape to the isotherm is typical of a Type II or Type IV isotherm, the difference being whether the mass continues to increase as p approaches p_0 (Type II) or whether it levels off (Type IV) [4]. The isotherm in Fig. 2a reaches a limiting value of 2.1 μg at $p/p_0 = 1$, making it a Type IV isotherm. Note that a $GaPO_4$ crystal with no CNT film only adsorbs about 40 ng of toluene under the same experimental conditions.

Type IV isotherms are considered to reflect capillary condensation in porous solids with the upper limit of adsorption mainly governed by the total pore volume [4]. An effective pore volume can therefore be estimated as 2.4×10^{-6} cm^3, by using the bulk density of toluene (0.87 g/cm^3). The total volume of the VACNT film is calculated by assuming it to be a cylindrical disk, with a diameter of 7 mm and a thickness of 3 μm (measured by profilometry). The volume of the VACNT film is therefore about 120×10^{-6} cm^3, giving an effective porosity of 2.4/120 = 2%. The isotherm shows hysteresis between the adsorption and desorption sweeps, mainly at higher loadings. Varying the sweep parameters showed this hysteresis to be a robust feature of the isotherm. Adsorption hysteresis is commonly seen with porous materials [4].

At low pressures ($p/p_0 < 0.25$) the isotherm shows a power law dependence as indicated by a straight line on a log–log plot (see Fig. 2b). This behavior is consistent with the Freundlich model: $m = k\,(p/p_0)^{1/n}$, where m is the mass of adsorbate, and k and n are fitting parameters [4]. The parameters resulting from a fit of the Freundlich model to the isotherms in this low pressure region are summarized in Table 1 for the adsorbates investigated here [12]. The isotherms from the different adsorbates are very similar to each other. The theory of Brunauer, Emmett, and Teller (BET) is commonly used to analyse sigmoidal isotherms in the intermediate pressure regime:

$$\frac{p}{m \cdot (p_0 - p)} = \frac{1}{m_m \cdot c} + \frac{(c-1)}{m_m \cdot c}\left(\frac{p}{p_0}\right)$$

where m is the mass of adsorbate, m_m is the "monolayer" mass, and c is the BET constant [4]. The toluene isotherm is plotted on a BET plot in Fig. 2c. A straight line is obtained for $p/p_0 = 0.1–0.4$, indicating a good fit to the BET model in this pressure range. It is normal for the experimental isotherm to deviate from the BET model at higher pressures. The parameters resulting from a fit of the BET model to the isotherms in this intermediate pressure region are summarized in Table 1.

To understand better the adsorption mechanisms responsible for the experimentally observed isotherm, Monte Carlo simulations were performed on a model system consisting of a periodic array of (10, 10) single-walled CNTs. The simulated toluene adsorption isotherm is shown in Fig. 3. The simulated isotherm is similar to the experimentally observed one and consists of three consecutive processes, namely filling of the intratube micropores, monolayer coverage of the CNT external surface, and capillary condensation in the

Table 1 – Summary of the fitting parameters obtained from the Freundlich and BET fits to the isotherms for the investigated adsorbates.

Adsorbate	Freundlich[a]		BET[b]	
	k(μg)	n	m_m(μg)	c
Toluene	0.56	1.6	0.25	18
Hexane	0.45	2.3	0.19	14
Cyclohexane	0.52	2.0	0.22	15
2-Butanone	0.50	1.7	0.23	13

[a] for $p/p_0 < 0.25$.
[b] for $p/p_0 = 0.1–0.4$.

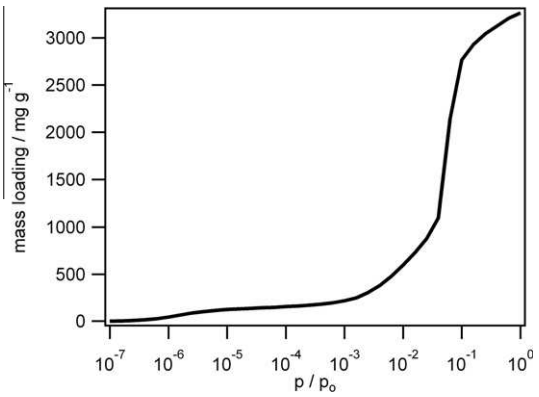

Fig. 3 – Simulated adsorption isotherm of toluene on a (10, 10) single-walled CNT with periodic boundary conditions.

intertube mesopores. At low pressures ($p/p_0 < \sim 10^{-4}$), toluene tends to firstly occupy the internal space of the CNT microchannels where the interactions between the toluene and the CNT wall are strongest (see Fig. 4a). The kinetic diameter of toluene is about 6 Å, which is half the size of the (10, 10) CNT channels. In this way, toluene can be packed in parallel along the channels. After saturation inside the CNT, toluene starts to adsorb on the outer surface of the CNT wall as the secondary site (Fig. 4b). In the pressure range up to $p/p_0 = \sim 10^{-2}$, a monolayer of toluene is formed densely about 3–4 Å above the CNT wall. The cylindrical structure of the toluene layer has a diameter of about 20 Å that allows approximately 8–10 molecules resident at the same longitude. At higher pressures, the condensation of toluene takes place in the mesopores between the CNTs, the size of which is 40 Å in this simulation (Fig. 4c). The density of all external toluene reaches a value of 0.82 g/cm^3, which is close to the density of liquid toluene (0.87 g/cm^3).

The use of the BET model to obtain meaningful monolayer capacities (and hence surface areas) for microporous materials is controversial [14]. Nevertheless, the simulations presented here clearly show a monolayer of toluene forming around the CNT and the BET model fits the experimentally observed isotherm well. BET surface areas are therefore calculated from the experimentally derived monolayer mass (m_m), as $S_{BET} = m_m N_A s/M$, where S_{BET} is the total BET surface area, m_m is the experimental monolayer mass (see Table 1), N_A is the Avogadro number, s is the molecular adsorption cross section, and M is the molecular mass [4]. The molecular adsorption cross section s is calculated from the molecular

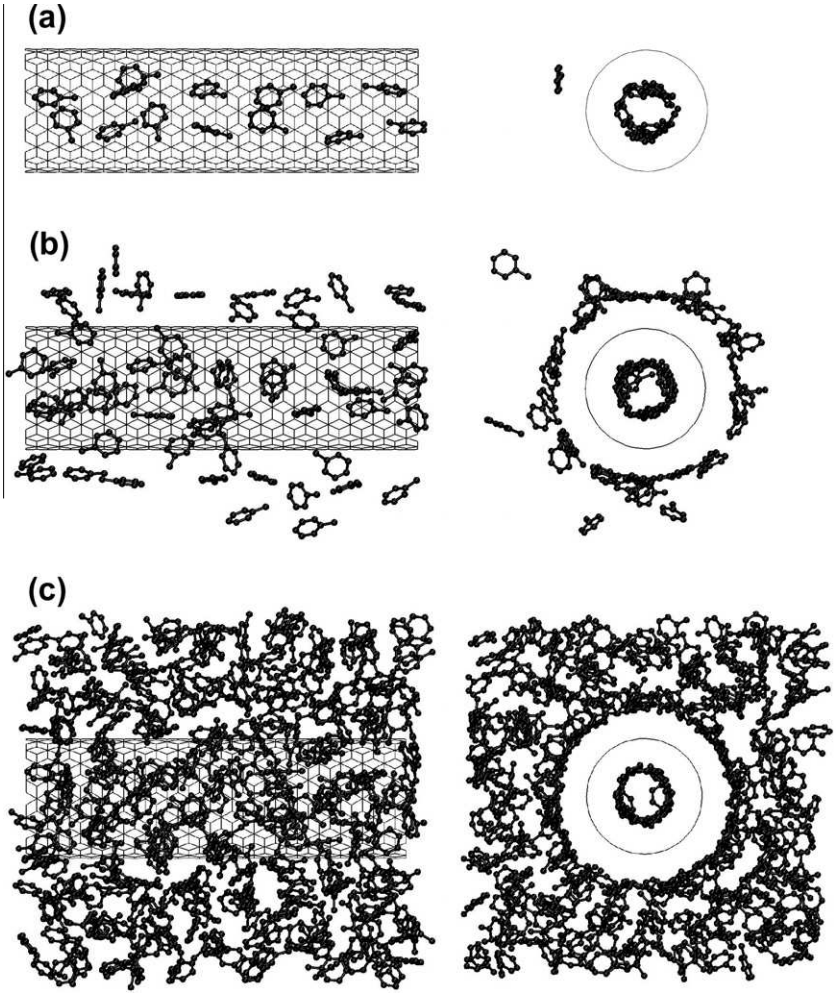

Fig. 4 – Simulation snapshots of toluene occupancy at (a) $p/p_0 = 10^{-4}$, (b) $p/p_0 = 10^{-2}$, and (c) $p/p_0 = 1$.

Table 2 – BET surface area analysis.

Adsorbate	M[a] (g/mol)	d[a] (nm)	s (nm^2)	S_{BET} (mm^2)
Toluene	92.2	0.476	0.178	290
Hexane	86.2	0.265	0.055	73
Cyclohexane	84.2	0.429	0.144	230
2-Butanone	72.1	0.275	0.059	110

[a] *Source:* Ref. [12].

diameter d as $s = \pi\, d^2/4$ [12]. The results of this analysis are summarized in Table 2. The total BET surface areas calculated for the different adsorbates used in this study range from 73 to 290 mm^2, with an average value of 180 ± 100 mm^2 (1σ). The variation in the BET parameters for the different adsorbates (see Table 1) is much less than the variation in the total BET surface areas, indicating that the isotherm is relatively insensitive to the identity of the adsorbate. This insensitivity of the isotherm comes in spite of the differences in the molecular mass and size of the adsorbates used in this study. The mass of the CNT film on the device is estimated from the frequency shift caused by film growth and is about 4.0 ± 0.3 μg. The specific surface area (SSA) is calculated by normalizing the total BET surface area by the mass of the film: 180 ± 100 mm^2/4.0 ± 0.3 μg = 45 ± 25 m^2/g. Reported measurements of SSA on bulk CNT materials range from about 40 to 600 m^2/g, which is somewhat less than the SSA reported on activated carbons (800–1100 m^2/g) [15].

Pore volumes measured on bulk CNT samples using organic vapor adsorbates were found by Agnihotri and co-workers to be about half that measured using nitrogen as an adsorbate [12]. The CNT films studied here are composed of multiwalled CNTs [2]. The inner walls of the CNT add mass to the film but do not add surface area. Therefore, the SSA can be increased by generating a film of CNTs with less or no internal walls. The 7 mm diameter CNT film patch has a projected area of 38 mm^2; the average BET surface area is about five times larger than this. Coupled with the previously measured 2% porosity, this suggests that it is possible that only the CNTs near the surface of the film are contributing to the vapor adsorption. That is, the vapors cannot penetrate deeply into the film and the film is acting more like a roughened surface. However, lowering the CNT growth time during fabrication to 5 min. produced a device with a 3.1 μg film mass and a toluene S_{BET} of 240 mm^2 (compared with 4.0 μg and 290 mm^2 obtained with the 20 min. growth time). Ideally the surface roughening picture would produce a S_{BET} that was insensitive to growth time.

The effective density of the film is 4.0 μg/120×10^{-6} cm^3 = 0.03g/cm^3. The density of bulk graphite is about 2 g/cm^3, giving a film density of about 2% of the bulk graphite density, indicating a large "void" volume in the film (greater than 90%). This void volume, however, seems to be largely inaccessible to the adsorbate. Therefore, a large increase in SSA can also possibly be achieved by making this void volume accessible. Blockages to the void volume inside the core of the CNTs could be from end caps, bamboo structure, or embedded catalyst particles. There could also be blockages to the void volume between the CNTs from the overall morphology of the film. Optimization of the film microstructure is clearly needed to achieve a higher SSA. The main parameters governing this microstructure optimization are the substrate preparation, catalyst composition, and CNT growth conditions. Post-growth processing may also be used, such as opening the CNT ends by an oxygen plasma or the removal of catalyst particle blockages by acid treatment.

4. Summary

Organic vapor adsorption isotherms are successfully measured on in situ grown VACNT films using piezoelectric $GaPO_4$ crystals as mass sensing substrates. The isotherms are Type IV and show adsorption/desorption hysteresis, consistent with a porous material. An effective porosity of 2% is calculated. At low pressures ($p/p_0 < 0.25$) the isotherm is well fit by the Freundlich model and at intermediate pressures ($p/p_0 = 0.1$–0.4) by the BET model. Monte Carlo simulations show three consecutive adsorption processes: filling of the intratube micropores at low pressures, monolayer coverage of the CNT external surface at intermediate pressures, and capillary condensation in the intertube mesopores at high pressures. The simulation results validate the use of the BET model for surface area analysis in the experimental system. The average total BET surface area is calculated to be 180 ± 100 mm^2 and the specific BET surface area is estimated to be 45 ± 25 m^2/g. Further engineering of the film structure should lead to increases in the total surface area and specific surface area, and are needed before the envisioned applications of these films can be realized.

Acknowledgements

Funding for this work was provided by the National Research Council Canada. We gratefully acknowledge the technical support from the NINT Cleanroom staff in keeping the reactors and other key equipment operational. Electron microscopy was performed in the NINT Electron Microscopy Facilities, with assistance from Daniel Salamon.

REFERENCES

[1] Joselevich E, Dai H, Liu J, Hata K, Windle AH. Carbon nanotube synthesis and organization. Top Appl Phys 2008;111:101–64.
[2] Bosnick K, Dai L. Growth kinetics in a large-bore vertically aligned carbon nanotube film deposition process. J Phys Chem C 2010;114(16):7226–30.
[3] Dai L, Wang P, Bosnick K. Large-scale production and metrology of vertically aligned carbon nanotube films. J Vac Sci Tech A 2009;27(4):1071–5.

[4] Shaw DJ. Introduction to colloid and surface chemistry. 4th ed. Oxford UK: Butterworth; 1992. pp. 115–50.
[5] Bourgeois A, Turcant Y, Walsh Ch, Defranoux Ch. Ellipsometry porosimetry (EP): thin film porosimetry by coupling an adsorption setting with an optical measurement, highlights on additional adsorption results. Adsorption 2008;14(4–5):457–65.
[6] Rouessac V, van der Lee A, Bosc F, Durand J, Ayral A. Three characterization techniques coupled with adsorption for studying the nanoporosity of supported films and membranes. Micropor Mesopor Mat 2008;111(1–3): 417–28.
[7] Yang ZP, Ci L, Bur JA, Lin SY, Ajayan PM. Experimental observation of an extremely dark material made by a low-density nanotube array. Nano Lett 2008;8(2):446–51.
[8] Silverstein MS, Bauer BJ, Hedden RC, Lee HJ, Landes BG. SANS and XRR porosimetry of a polyphenylene low-k dielectric. Macromolecules 2006;39(8):2998–3006.
[9] Borrás A, Sánchez-Valencia JR, Garrido-Molinero J, Barranco A, González-Elipe AR. Porosity and microstructure of plasma deposited TiO_2 thin films. Micropor Mesopor Mat 2009; 118(1–3):314–24.
[10] Haines J, Cambon O, Keen DA, Tucker MG, Dove MT. Structural disorder and loss of piezoelectric properties in alpha-quartz at high temperature. Appl Phys Lett 2002;81(16):2968–70.
[11] Elam JW, Pellin MJ. $GaPO_4$ sensors for gravimetric monitoring during atomic layer deposition at high temperatures. Anal Chem 2005;77(11):3531–5.
[12] Agnihotri S, Rood MJ, Rostam-Ababdi M. Adsorption equilibrium of organic vapors on single-walled carbon nanotubes. Carbon 2005;43(11):2379–88.
[13] Frenkel D, Smit B. Understanding molecular simulation: from algorithms to applications. 2nd ed. San Diego CA: Academic Press; 2002.
[14] Walton KS, Snurr RQ. Applicability of the BET method for determining surface areas of microporous metal-organic frameworks. J Am Chem Soc 2007;129(27):8552–6.
[15] Pan P, Xing B. Adsorption mechanisms of organic chemicals on carbon nanotubes. Environ Sci Technol 2008;42(24):9005–13.